Supplemental Information for:

Exploring the Influence of H-Bonding and Ligand Constraints on Thiolate Ligated Non-Heme Iron Mediated Dioxygen Activation

Maike N. Lundahl,[a] Maria B. Greiner,[a] Marc C. Piquette,[b] Paige M. Gannon, [a] Werner Kaminsky[†a] and Julie A. Kovacs*[a]

[a]*Department of Chemistry, University of Washington, Campus Box 351700 Seattle, WA 98195, USA.*

[b]*Department of Chemistry, Tufts University, 62 Talbot Avenue, Medford, Massachusetts 02155, United States*

EXPERIMENTAL PROCEDURES

General Methods. Reagents purchased from commercial vendors were of the highest purity available and used without further purification. [$Fe^{II}(S_2^{Me2}N_3(Pr,Pr)$] (**1**) and [$Fe^{III}(S_2^{Me2}N_3(Pr,Pr)]PF_6$ (**3**) were synthesized as previously described.[1, 2] Methanol (MeOH) was distilled over magnesium turnings and iodine and degassed prior to use. Un-stabilized tetrahydrofuran (THF) was rigorously degassed and purified using solvent purification columns housed in a custom stainless-steel cabinet, dispensed via a stainless steel Schlenk line (GlassContour). All manipulations were performed using Schlenk line techniques or under an N_2 atmosphere in a glovebox.

Evans Method of [$Fe^{II}(S_2^{Me2}N_3(Pr,Pr)$] (1). ^{1}H-NMR spectra were recorded on Bruker AV 301 FT-NMR spectrometers and are referenced to residual protio-solvent. Chemical shifts are reported in ppm. The magnetic moment of **1** was determined to be μ_{eff} = 4.69 B.M (MeOH), and μ_{eff} =4.08 B.M. (THF) using the Evans method.

Kinetic Measurements. Solutions were prepared in a N_2-filled anaerobic glove-box ([O_2] <1 ppm) and placed in Hamilton gastight® syringes equipped with three-way valves. Time-resolved spectra (350−820 nm) were acquired at low temperatures using a TgK Scientific (U.K.) CSF-61DX2 Multi-Mixing CryoStopped-Flow Instrument equipped with a tungsten visible light source. The stopped-flow instrument is equipped with PEEK tubing fitted inside stainless-steel plumbing, a 1.00 cm^3 quartz mixing cell, and an anaerobic kit purged with an inert gas. The temperature in the mixing cell was maintained to ± 0.1 °C, and the mixing time was 2-3 ms. All flow lines of the instrument were extensively washed with degassed, anhydrous THF or MeOH before charging the driving syringes with solutions containing the reactants. The reactions were studied by rapid scanning

spectrophotometry under pseudo-first order conditions with excess oxygen or superoxide. Saturated solutions of O_2 were prepared as described below. The O_2 concentration was assumed not to change upon cooling, given that the system is closed, and the solutions were not in contact with the gas phase (small variations in the solvent density were not taken into account). Dilutions of the O_2-saturated solvent were performed anaerobically to obtain the desired [O_2]. Potassium superoxide solutions were prepared as described below. All concentrations reported in stopped-flow experiments refer to the "after mixing" conditions. Experiments were performed in single-mixing mode, with a 1:1 (v/v) mixing ratio. A series of three or four measurements with outliers (Grubbs test, 95 % confidence interval)[3] removed prior to data averaging gave an acceptable standard deviation (within 10%). Rates reported for the oxygen dependence are the average of at least three different experiments. Data analysis was performed with Kinetic Studio software from TgK Scientific.[4] Data was fit at a single wavelength (523.5 nm) using the following equation:

$$A_t = A_\infty - (A_\infty - A_0)e^{-k_{obs}t} \quad (1)$$

The reaction order with respect to O_2 was determined by varying the O_2 concentration over the range of 1.975 mM to 3.95 mM in THF, and 2.55 mM to 4.25 mM in MeOH, while maintaining a constant Fe(II) concentration (0.1 mM).

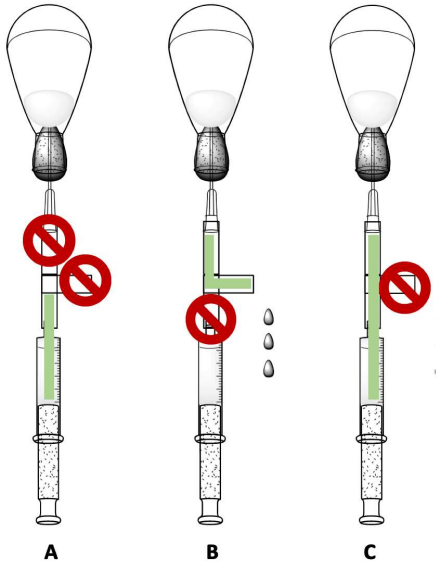

Kinetics for the formation of **2** via an alternate route involving KO_2 + Fe(III)-**3** were monitored at λ= 523 nm under pseudo first order

conditions with excess KO_2 (solubilized with Kryptofix ® 222) using a TgK stopped-flow instrument and CCD detector. Constant ionic strength (0.01 M) conditions were maintained by adding an appropriate amount of Bu_4NPF_6. Kinetic traces were fit to the single exponential of eqn (1) with very small residuals (Figure S8).[4] Data was analyzed using Grubb's test[3] providing a 95% confidence level.

Preparation of Saturated Dioxygen Solutions. Degassed solvent (MeOH or THF) was added to a round bottom flask fitted with a septum cap under a nitrogen atmosphere in the glovebox. Dry O_2 (from a gas cylinder) was bubbled through the solvent at 1 atm for 15 min. The solution was then allowed to equilibrate over 15 minutes at 25 °C in a temperature-controlled water bath. The concentration of O_2 was taken as 8.5 mM in MeOH, and 7.9 mM in THF both at 25 °C.[5] To load the syringe in preparation for stopped-flow experiments, the flask was inverted and a gastight syringe equipped with a 3-way valve and needle was inserted through the septum (Position A in Figure on the right). The valve was then turned to allow the saturated solution to flow through the open arm of the 3-way valve, leaving no headspace in the needle (Position B). The valve was then closed, and the dioxygen solution drawn into the syringe (Position C).

Dilution of Dioxygen Solutions. Dilutions of the O_2-saturated solvent were performed anaerobically by attaching a second syringe filled with an excess of an appropriate

quantity of deoxygenated solvent to the open arm of the 3-way valve (Position D in Figure below). Air bubbles trapped in the valve by this process were purged by flowing the excess solvent through the needle down to the quantity of solvent necessary for the desired O_2 concentration (Position E). The valve was then turned to allow the two needles to communicate, and the saturated O_2 solution was drawn into the deoxygenated solvent until the desired O_2 concentration is met (Position F). The dilute O_2 solution was then allowed to equilibrate for 30 min after which time it was ready for use. This dilution process can be repeated in the same manner if it is not practical to attain the desired O_2 concentration via one dilution.

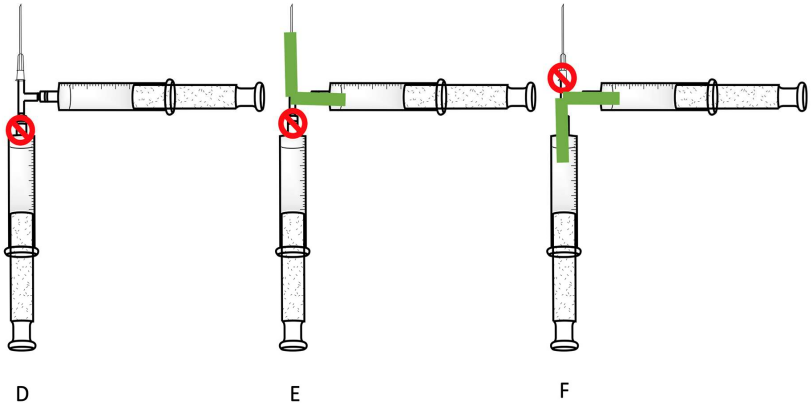

Preparation of Potassium Superoxide Solutions. A very fine powder of KO_2 was weighed out on an analytical balance, and then 1 eq. of Kryptofix®222 was added to solubilize the KO_2 in THF. The solution was vigorously stirred at RT in a glovebox for at least 20 mins and used within 6 hrs of preparation. An appropriate amount of Bu4NPF6 (9.8 – 17.8 mM pre-mix concentration) was added to maintain a constant ionic strength of 10 mM (post-mix concentration). Kinetic traces were fit to the single exponential of eqn (1) with very small residuals (Figure S14).

Computational Details. Calculations were performed using the ORCA v. 5.0.4 quantum chemistry package developed by Neese and coworkers,[6] and employed a polarized triple-

zeta def2-TZVP basis set, the def2/J auxiliary basis set for Coulomb fitting, and the atom-pairwise dispersion correction of Grimme (D3BJ).[7] Tight convergence criteria were required for self-consistent field (SCF) solutions. The DEFGRID3 integration grid size, and the conductor-like polarizable continuum model with the dielectric constant ε = 7.25 for tetrahydrofuran solvent (CPCM(THF)), or the dielectric constant ε = 32.63 for methanol solvent (CPCM(MeOH)), were used for geometry optimizations.[8] Geometry optimizations and analytical frequency calculations were performed using the B3LYP functional, with the resolution of identity (RI) chain-of-spheres (RIJCOSX) approximation,[9, 10] and initiated from the crystallographic coordinates when available. Analytical frequency calculations were performed on all optimized structures to determine whether the obtained stationary points corresponded to local minima.

Calculations for the Fe(III)-superoxo complex, [$Fe^{III}(S_2^{Me2}N_3(Pr,Pr)(O_2)$] (**4**) employed the broken-symmetry formalism to model coupled paramagnetic sites. The previously reported[1] DFT optimized structure of superoxo [$Fe^{III}(S_2^{Me2}N_3(Pr,Pr))(O_2)$] (**2**) was used as a starting point for the calculated structure in a polarizable continuum model in MeOH. Hybrid time-dependent DFT (TD-DFT) calculations employed the RIJCOSX and the Tamm-Dancoff approximations (TDA).[11, 12] The Fermi level, i.e., the halfway between the calculated HOMO and LUMO energies, was set to 0 eV in molecular orbital (MO) analysis. Excited states from TD-DFT calculations were analyzed using Natural Transition orbitals (NTOs) and by visualizing their difference densities between the ground and excited states. Canonical molecular orbital isosurfaces and natural transition orbitals in the TD-DFT calculations were visualized at an isovalue of 0.08 a_0^3 using UCSF Chimera.[13]

X-ray Crystallographic Structure Determination. A yellow needle, measuring 0.36 x 0.04 x 0.03 mm^3 was mounted on a loop with oil. Data was collected at -173°C on a Bruker APEX II single crystal X-ray diffractometer, Mo-radiation, equipped with a Miracol X-ray optical collimator.

Crystal-to-detector distance was 40 mm and exposure time was 20 seconds per frame for all sets. The scan width was 0.5°. Data collection was 100% complete to 25° in ϑ. A total of 20760 reflections were collected covering the indices, -25<=h<=25, -16<=k<=16, -12<=l<=12. 5450 reflections were symmetry independent and the R_{int} = 0.0595 indicated that the data was good. Indexing and unit cell refinement indicated a primitive orthorhombic lattice. The space group was found to be P c a 2_1 (No. 29).

The data was integrated and scaled using SAINT, SADABS within the APEX2 software package by Bruker.[14] Solution by direct methods (SHELXT[15, 16]) produced a complete heavy atom phasing model consistent with the proposed structure. The structure was completed by difference Fourier synthesis with SHELXL.[16, 17] Scattering factors are from Waasmair and Kirfel.[18] Hydrogen atoms were placed in geometrically idealized positions and constrained to ride on their parent atoms with C---H distances in the range 0.95-1.00 Angstrom. Isotropic thermal parameters U_{eq} were fixed such that they were 1.2U_{eq} of their parent atom Ueq for CH's and 1.5U_{eq} of their parent atom U_{eq} in case of methyl groups. All non-hydrogen atoms were refined anisotropically by full-matrix least-squares.

Crystallographic data is presented as ray-traced ORTEP plot.[19] The structural overlays (Fig. 11, main text) were generated using BIOVIA Discovery Studio software.[20]

Derivation of the Rate Expression. The general kinetic scheme, eqn (2), and a derivation of the rate expression is shown in eqns (3) – (10).[21] This derivation uses mass balance (eqn (4)), and assumes that the concentration of **2** at any given time, $[FeO_2]_t$, is equal to the initial concentration of **1**, $[Fe^{II}]_0$, minus the concentration of **1** at any given

$$Fe^{II} + O_2 \underset{k_{off}}{\overset{k_{on}}{\rightleftharpoons}} Fe^{III}O_2 \qquad (2)$$

$$\frac{d[Fe^{III}O_2]}{dt} = k_{on}[Fe^{II}]_t[O_2] - k_{off}[Fe^{III}O_2]_t \qquad (3)$$

$$[Fe^{II}]_0 = [Fe^{II}]_t + [Fe^{III}O_2]_t \qquad (4)$$

$$[Fe^{III}O_2]_t = [Fe^{II}]_0 - [Fe^{II}]_t \qquad (5)$$

$$\frac{d[Fe^{III}O_2]}{dt} = k_{on}[Fe^{II}]_t[O_2] - k_{off}([Fe^{II}]_0 - [Fe^{II}]_t) \qquad (6)$$

$$= k_{on}[Fe^{II}]_t[O_2] + k_{off}[Fe^{II}]_t - k_{off}[Fe^{II}]_0 \qquad (7)$$

$$= [Fe^{II}]_t (k_{on}[O_2] + k_{off}) - k_{off}[Fe^{II}]_0 \qquad (8)$$

$$\frac{d[Fe^{III}O_2]}{dt} = k_{obs}[Fe^{II}]_t - C \qquad (9)$$

$$k_{obs} = k_{on}[O_2] + k_{off} \qquad (10)$$

time, $[Fe^{II}]_t$. Solving for the unknown concentration of superoxo **2**, $[FeO_2]_t$ in terms of $[Fe^{II}]_0$ and $[Fe^{II}]_t$ (eqn (5)), and substituting this into eqn (3), we obtain eqn (6), which simplifies to eqn (8). Under pseudo first order conditions with excess O_2 the rate expression is that of eqn (9), with k_{obs} defined in eqn (10). The term $k_{off}[Fe^{II}]_0$ is a constant, C (eqn (9)), that does not change with time, therefore it does not affect the measured rate constant k_{obs}. The magnitude of C is small relative to the other terms when working with sub-mM concentrations of $[Fe^{II}]_0$, and thus it can be dropped from eqn (9).[21] For a reversible process under pseudo first-order conditions with excess O_2, k_{obs}

would be dependent on both k_{off} and k_{on},[21] wherein the former can be obtained from the intercept, and the latter from the slope.

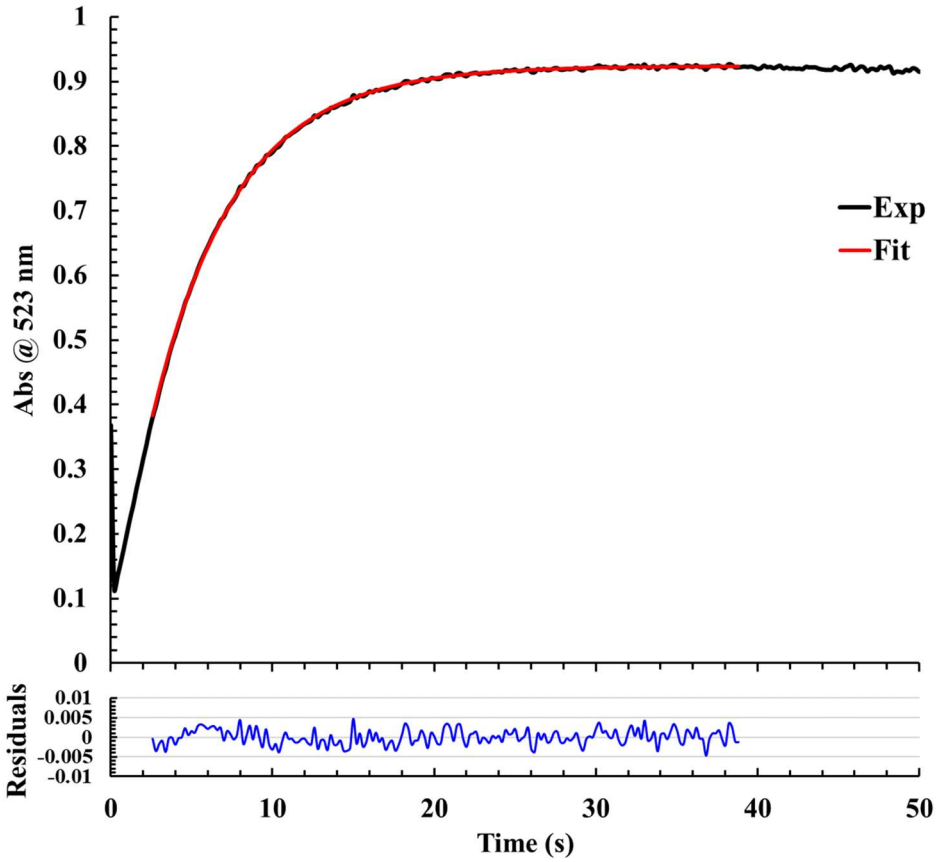

Figure S1. Kinetic trace at λ = 523 nm acquired -40 ˚C with [**1**] = 0.25 mM and [O_2] = 4.0 mM in THF (concentrations in the mixing cell are given). The experimental trace is shown in black; the pseudo-first order fit is shown in red; residuals in blue are appended to the bottom of the graph.

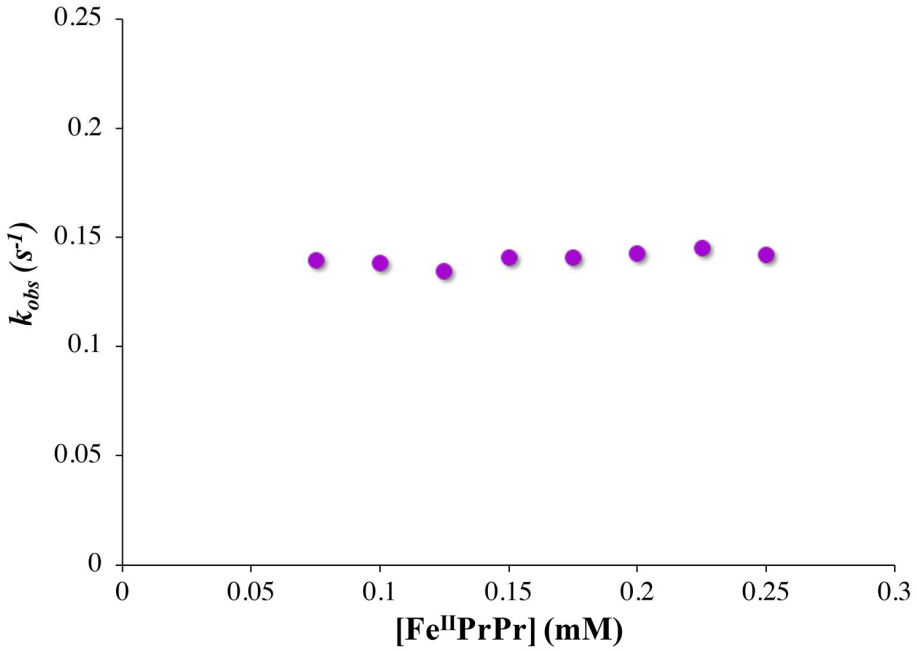

Figure S2. Plot of observed rate constants (k_{obs}) for the formation of Fe^{III}-superoxo **2** versus [Fe^{II}($S_2^{Me2}N_3$(Pr,Pr)] (**1**) concentration at -40 ˚C in THF. [O_2] after mixing = 3.95 mM.

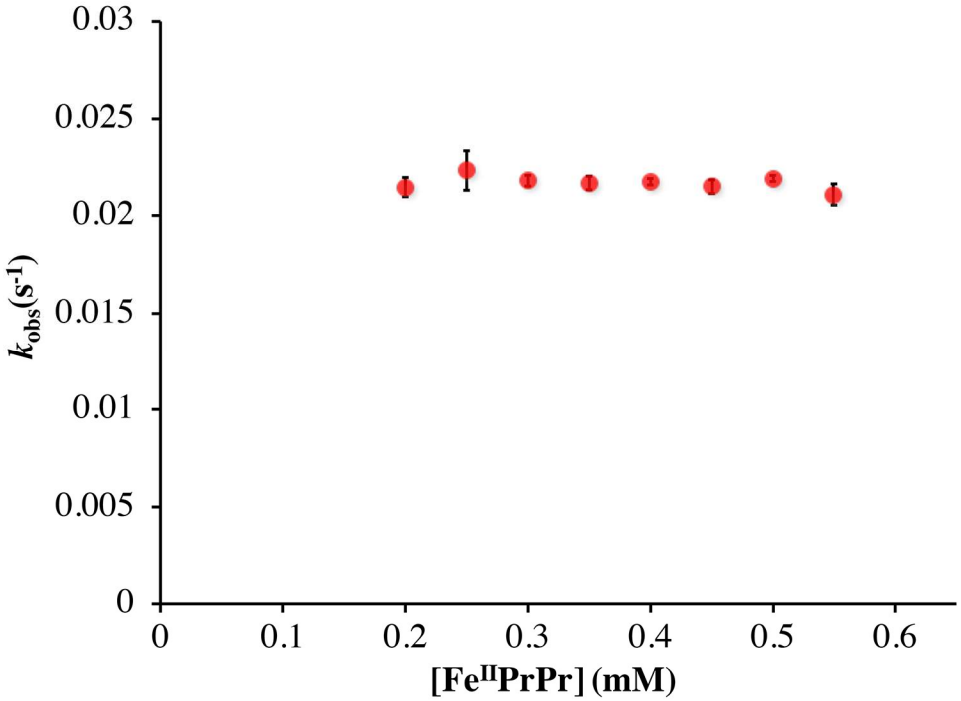

Figure S3. Plot of observed rate constants (k_{obs}) for the formation of Fe^{III}-superoxo **2** versus the concentration of [Fe^{II}($S_2^{Me2}N_3$(Pr,Pr)] (**1**) at 0 ˚C in MeOH. [O_2] after mixing = 4.25 mM.

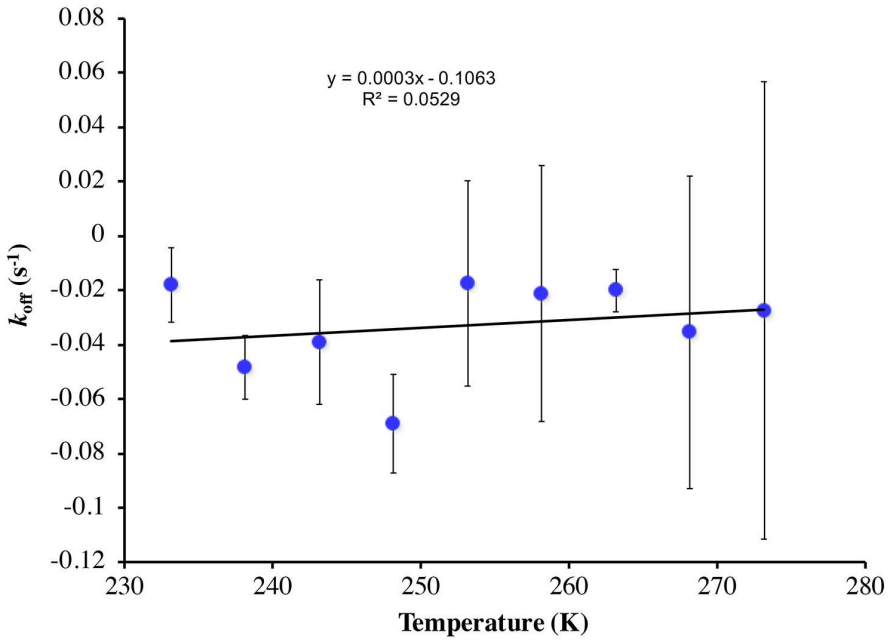

Figure S4. The dissociation rate constant, k_{off}, obtained from the y-intercept of the k_{obs} vs $[O_2]$ plots of Figure 3 (main text), does not correlate with temperature in THF. This, coupled with the ~zero intercept of Figure 3 would be consistent with irreversible O_2 binding to **1** in this solvent.

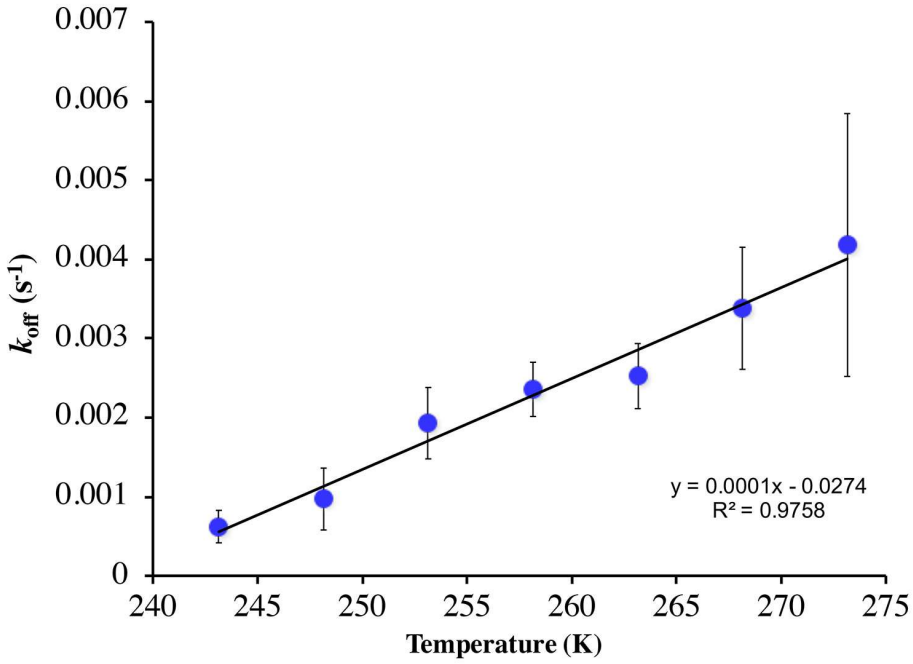

Figure S5. Correlation between temperature and rate constants for O_2 release from superoxo **2**, k_{off}, in MeOH. Dissociation rate constants, k_{off}, were obtained from the y-intercept of the k_{obs} vs $[O_2]$ plots (Figure 4 of main text)

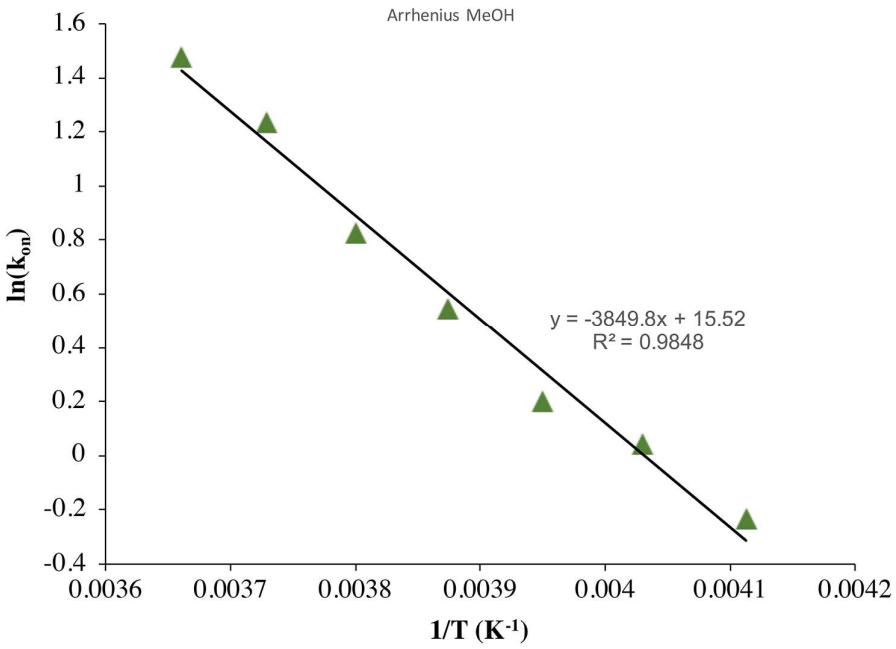

Figure S6. Arrhenius plot for O_2 binding to **1** in MeOH, from which activation parameter E_a= 32(2) kJ mol^{-1} was obtained.

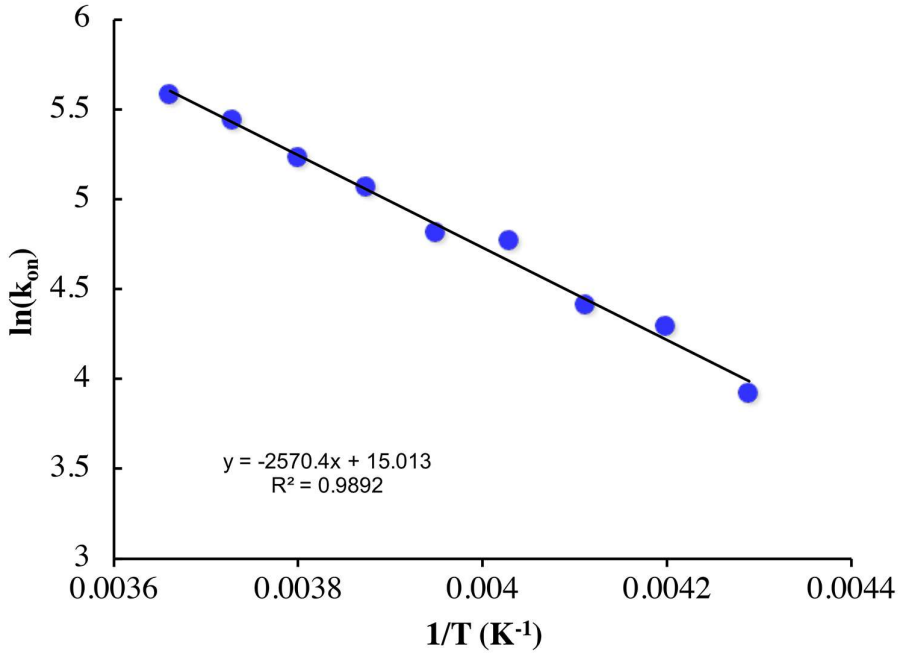

Figure S7. Arrhenius plot for O_2 binding to **1** in THF, from which activation parameter E_a= 21.4(8) kJ mol^{-1} was obtained.

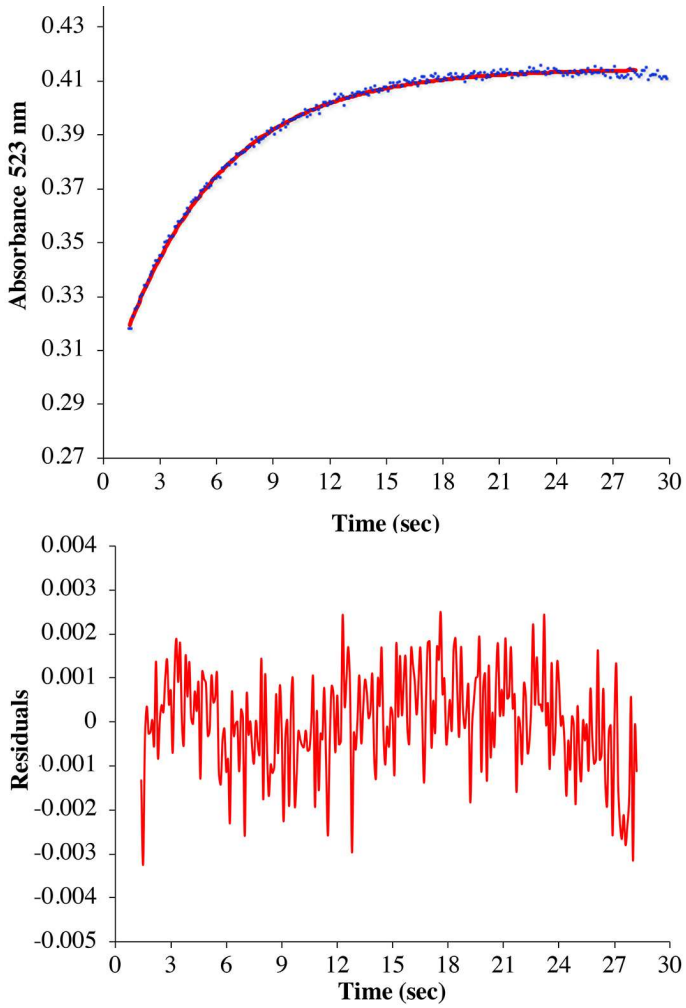

Figure S8. Kinetic trace for superoxide (KO_2) binding to **3** monitored at λ = 523 nm with [**1**] = 0.1 mM and [KO_2] = 5.0 mM in THF at -40 ˚C under a constant ionic strength of 0.01 M with added Bu_4NPF_6 (concentrations listed are after mixing in the stopped-flow cell). The experimental data points are shown in blue; the pseudo-first order fit to eqn (1) of the main text is shown in red; residuals in red are appended to the bottom of the graph.

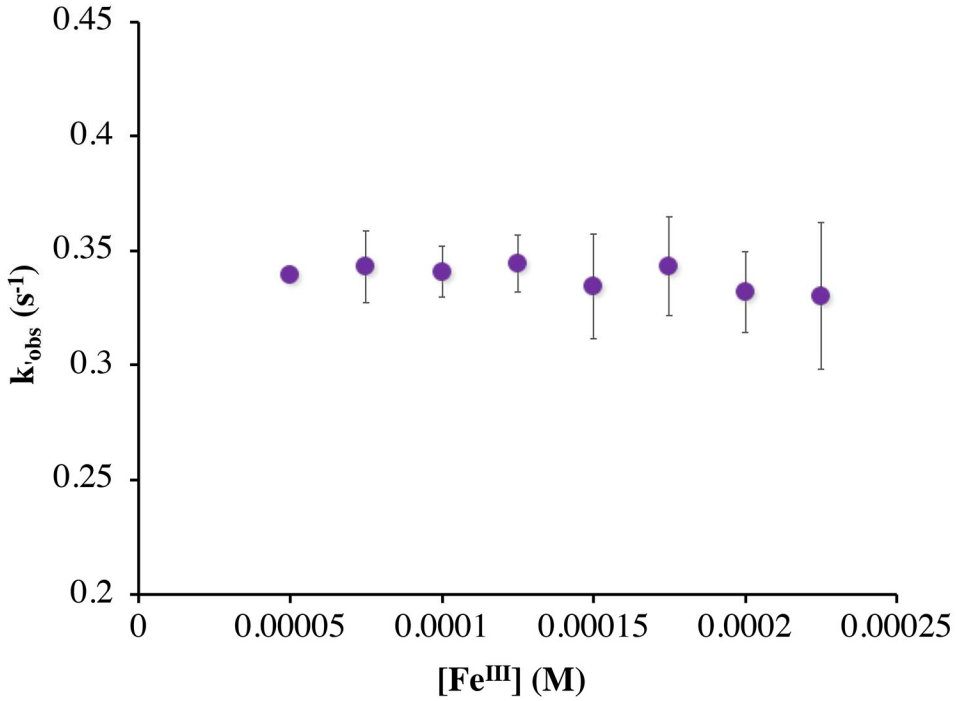

Figure S9. Zero order dependence of k_{obs} on Fe(III) concentration under pseudo first order conditions with excess KO_2 (5 mM). This would be consistent with 1st order dependence on Fe(III) overall.

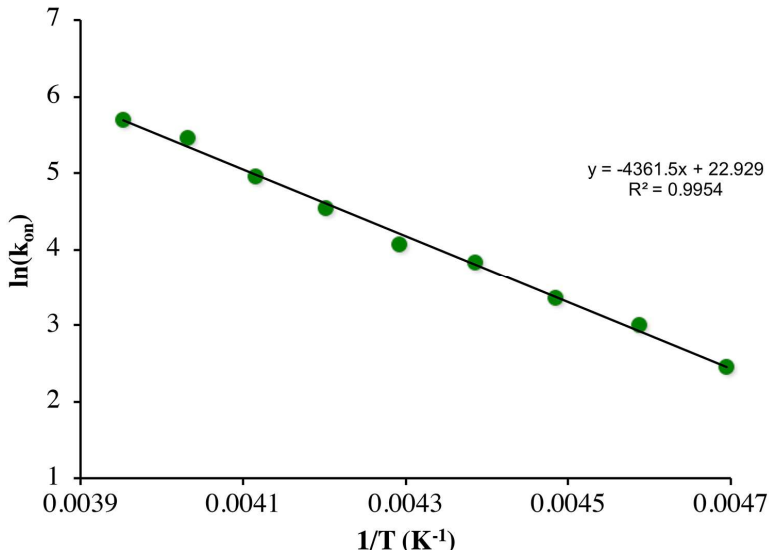

Figure S10. Arrhenius plot for superoxide (KO_2 solubilized with KryptoFix) binding to Fe(III)-**3** in THF.

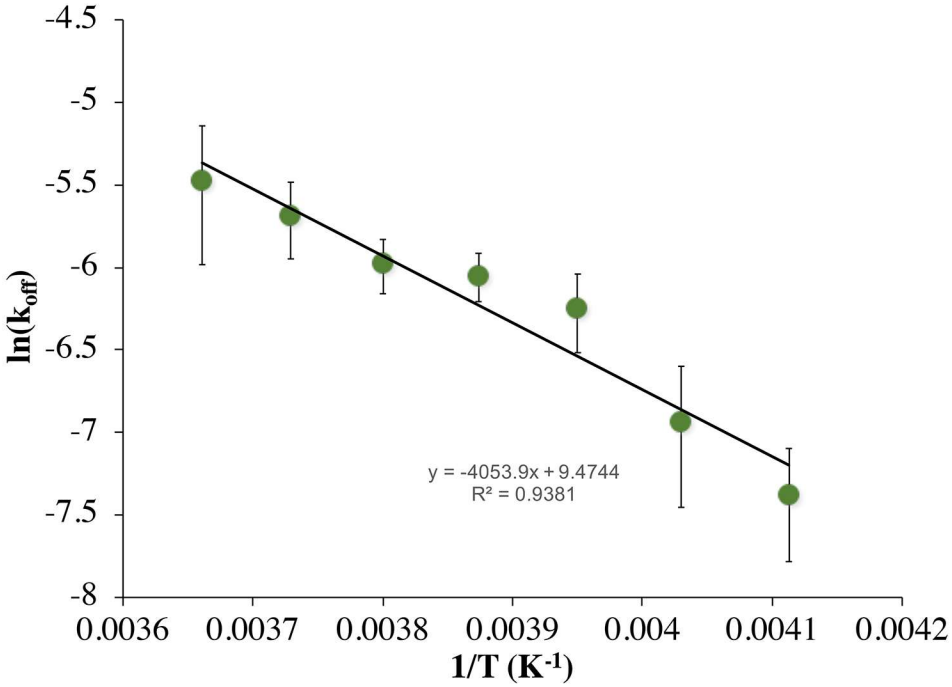

Figure S11. Arrhenius plot for O_2 release from superoxo **2** in MeOH, from which the activation parameter E_a= 34(4) kJ mol^{-1} was obtained.

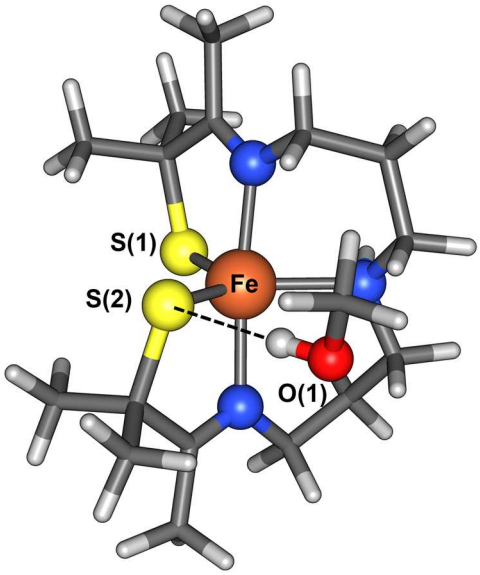

Figure S12. DFT optimized structure of [$Fe^{II}(S_2^{Me2}N_3(Pr,Pr)$]•••H-OMe (**1**) containing a MeOH solvent molecule H-bonded to one of the thiolate sulfurs, S(2). Calculated MeO(1)-H•••S(2) distance is 2.224 Å (see Table S10).

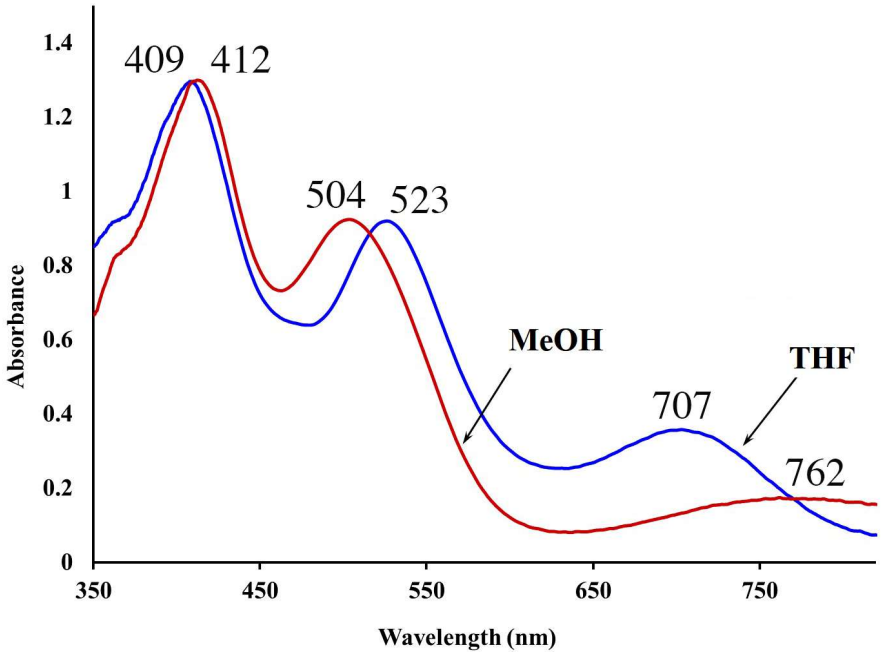

Figure S13. Experimental electronic absorption spectrum of Fe^{III}-superoxo **2** (0.25 mM) in THF vs MeOH.

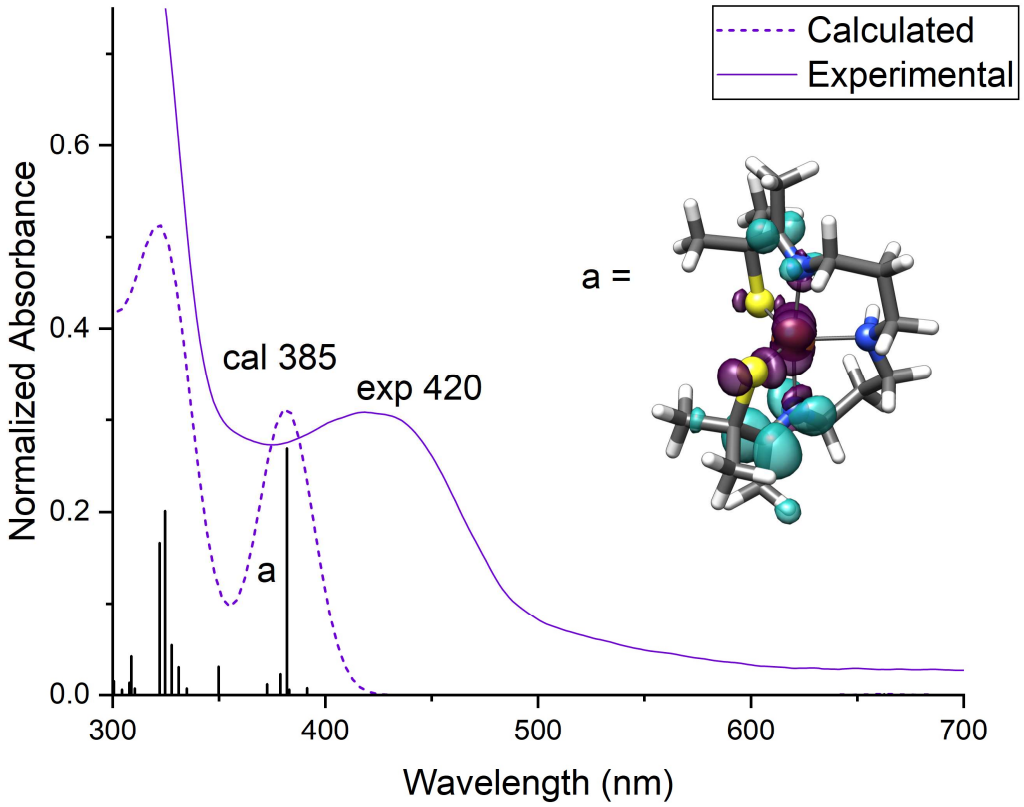

Figure S14. Time-dependent DFT (TD-DFT) calculated electronic absorption spectrum of [$Fe^{II}(S_2{}^{Me2}N_3(Pr,Pr)$] (**1**) modeled in THF (purple dashed line) overlaid with the experimental spectra (purple solid line). The computed transition of interest (black vertical sticks, a) is depicted with an electron difference density map where purple regions indicated electron density loss and the teal regions gain in electron density.

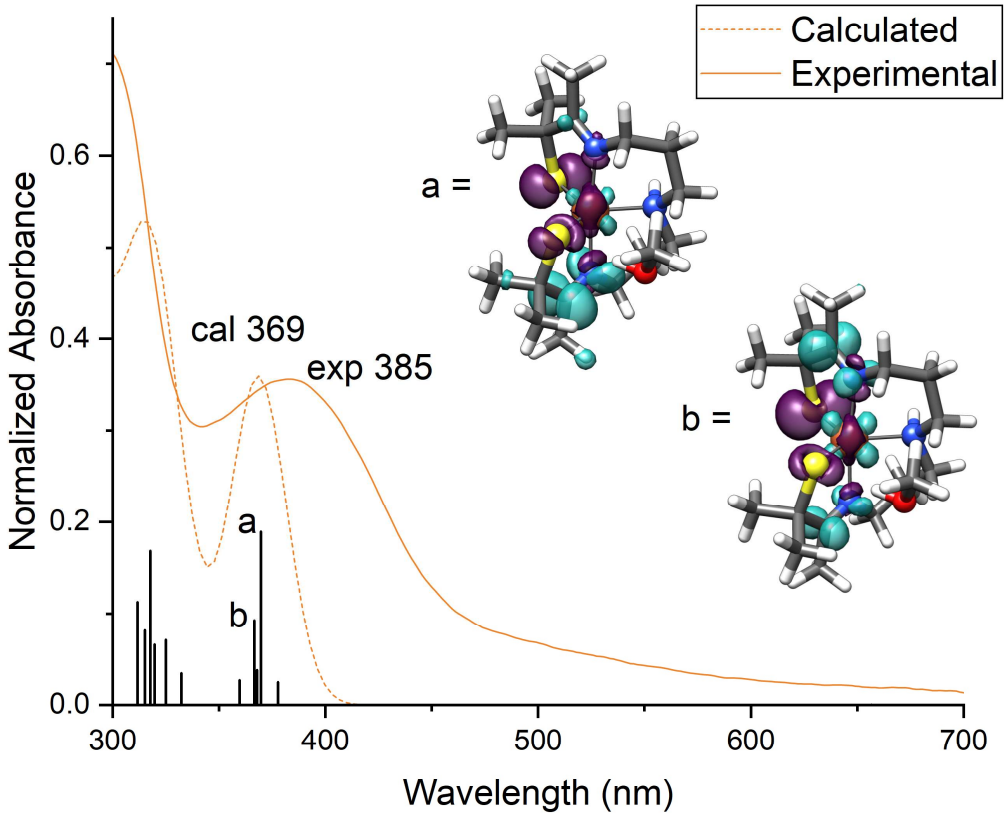

Figure S15. Time-dependent DFT (TD-DFT) calculated electronic absorption spectrum of [$Fe^{II}(S_2^{Me2}N_3(Pr,Pr)$] (**1**) modeled in MeOH (purple dashed line) overlaid with the experimental spectra (purple solid line) A MeOH solvent molecule H-bonded to one of the thiolate sulfurs causes the S→Fe charge transfer band to blue shift relative to that shown in Figure S13. The computed transition of interest (black vertical sticks, a & b) is depicted with an electron difference density map where purple regions indicated electron density loss and the teal regions gain in electron density.

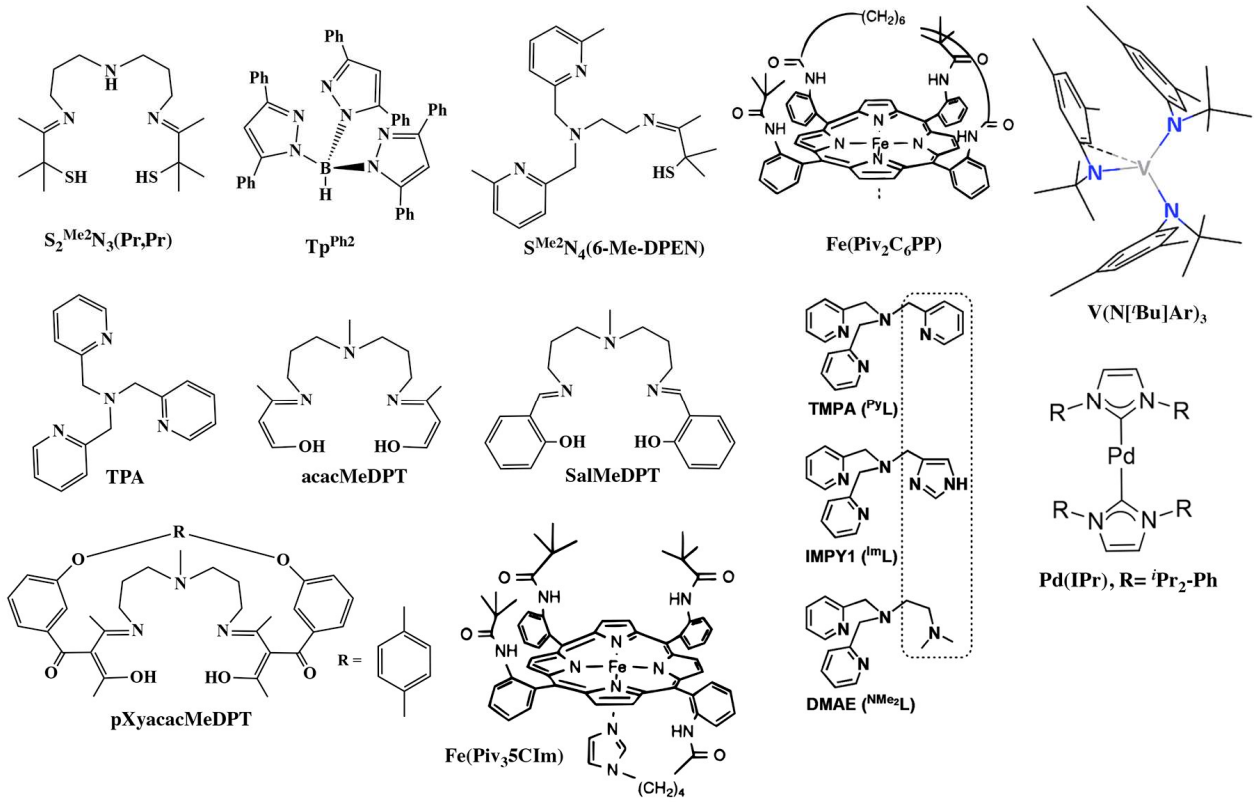

Figure S16. Chemdraw depiction of the ligands in Table 2 of main text.

Table S1. Temperature-dependent pseudo 1st order rate constants for the reaction between **1** ($[\mathbf{1}]_0$ = 0.25 mM) and O_2 in THF. All reported concentrations are after mixing in the stopped-flow cell.

Temperature (˚C)	$[O_2]$ (mM)	k_{obs} (s^{-1})
0	1.975	0.534(6)
	2.37	0.586(7)
	2.765	0.651(1)
	3.4	0.912(1)
	3.95	1.02(2)
-5	1.975	0.434(13)
	2.37	0.514(8)
	2.765	0.593(9)
	3.4	0.709(10)
	3.95	0.907(9)
-10	1.975	0.345(73)
	2.37	0.421(21)
	2.765	0.496(72)
	3.4	0.618(12)
	3.95	0.711(61)
-15	1.975	0.300(4)
	2.37	0.364(5)
	2.765	0.406(1)
	3.4	0.487(11)
	3.95	0.630(8)
-20	1.975	0.243(9)
	2.37	0.265(10)
	2.765	0.310(4)
	3.4	0.382(4)
	3.95	0.486(3)
-25	1.975	0.157(1)
	2.37	0.216(1)
	2.765	0.259(3)
	3.4	0.317(6)
	3.95	0.399(7)
-30	1.975	0.109(7)
	2.37	0.167(16)
	2.765	0.197(4)
	3.4	0.236(11)
	3.95	0.281(30)
-35	1.975	0.089(3)
	2.37	0.128(1)
	2.765	0.155(1)
	3.4	0.204(3)
	3.95	0.234(2)
-40	1.975	0.0767(20)
	2.37	0.110(8)
	2.765	0.118(23)
	3.4	0.147(13)
	3.95	0.183(11)

Table S2. Observed rate constants for the reaction between **1** ([**1**]$_0$ = 0.25 mM) and O_2 in MeOH. All reported concentrations are after mixing in the stopped-flow cell.

Temperature (˚C)	[O_2] (mM)	k_{obs} (s^{-1})
0	2.55	0.0152(6)
	2.975	0.0168(9)
	3.40	0.0199(8)
	3.825	0.021(1)
	4.25	0.0223(10)
-5	2.55	0.0121(1)
	2.975	0.0134(1)
	3.40	0.0154(1)
	3.825	0.0167(1)
	4.25	0.0178(2)
-10	2.55	0.00835(21)
	2.975	0.00919(76)
	3.40	0.0105(7)
	3.825	0.0112(1)
	4.25	0.0122(8)
-15	2.55	0.00674(17)
	2.98	0.00740(35)
	3.40	0.00834(10)
	3.825	0.00908(1)
	4.25	0.00957(2)
-20	2.55	0.00485(21)
	2.98	0.00575(53)
	3.40	0.00619(31)
	3.825	0.00658(15)
	4.25	0.00703(5)
-25	2.55	0.00369(1)
	2.98	0.00389(3)
	3.40	0.00470(17)
	3.825	0.00495(12)
	4.25	0.00539(27)
-30	2.55	0.00262(22)
	2.98	0.00301(2)
	3.40	0.00337(25)
	3.825	0.00354(2)
	4.25	0.00403(3)

Table S3. Temperature-dependent pseudo 1st order rate constants for the reaction between between **3** ($[\mathbf{3}]_0$ = 0.1 mM) and KO_2 solubilized with Kryptofix ® 222 in THF, under constant ionic strength (0.01 M) with 1.5-11.5 mM Bu_4NPF_6. All reported concentrations are after mixing in the stopped-flow cell.

Temperature (˚C)	$[O_2^{\bullet-}]$ (mM)	k_{obs} (s^{-1})
-20	1.0	0.393(1)
	2.0	0.642(12)
	3.0	0.959(87)
	4.0	1.226(30)
	5.0	1.592(12)
-25	1.0	0.322(13)
	2.0	0.442(14)
	3.0	0.637(26)
	4.0	0.936(65)
	5.0	1.251(63)
-30	1.0	0.225(4)
	2.0	0.296(5)
	3.0	0.431(51)
	4.0	0.562(20)
	5.0	0.801(31)
-35	1.0	0.172(5)
	2.0	0.195(4)
	3.0	0.288(7)
	4.0	0.406(36)
	5.0	0.539(33)
-40	1.0	0.123(5)
	2.0	0.159(16)
	3.0	0.226(18)
	4.0	0.288(83)
	5.0	0.351(9)
-45	1.0	0.092(8)
	2.0	0.117(3)
	3.0	0.166(5)
	4.0	0.204(23)
	5.0	0.278(13)
-50	1.0	0.0585(67)
	2.0	0.0761(57)
	3.0	0.110(5)
	4.0	0.133(5)
	5.0	0.174(11)
-55	1.0	0.0443(51)
	2.0	0.0588(10)
	3.0	0.0685(20)
	4.0	0.0992(23)
	5.0	0.125(10)
-60	1.0	0.0368(12)
	2.0	0.0488(13)
	3.0	0.0585(67)
	4.0	0.0694(7)
	5.0	0.0844(51)

Table S4. DFT calculated (using the B3LYP functional and def2-TZVP basis set) Mulliken charges for the optimized structure of [$Fe^{II}(S_2^{Me2}N_3(Pr,Pr)$] (**1**) in THF, $Fe^{II}(S_2^{Me2}N_3(Pr,Pr)$]•••H-OMe (**1•••H-OMe**) in MeOH and [$Fe^{III}(S_2^{Me2}N_3(Pr,Pr)(O_2)$] (**2**) in MeOH.

	Mulliken Charges		
Atom	**1** in THF	**1•••H-Ome** in MeOH	**2** in MeOH
Fe	+0.425	+0.447	+0.044
S(1)	-0.676	-0.678	-0.482
S(2)	-0.663	-0.662	-0.519
N(1)	-0.133	-0.132	+0.002
N(2)	-0.314	-0.318	-0.186
N(3)	-0.133	-0.149	+0.088
O(1)	NA	-0.525	NA
H(1)	NA	+0.295	NA

Table S5. Crystal data and structure refinement for [$Fe^{II}(S_2^{Me2}N_3(Pr,Pr)$]•••H-OMe (**1•••H-OMe**).

Identification code	mg2156_0m	
Empirical formula	C17 H35 Fe N3 O S2	
Formula weight	417.45	
Temperature	100(2) K	
Wavelength	0.71073 Å	
Crystal system	Orthorhombic	
Space group	P c a 2_1	
Unit cell dimensions	a = 19.3307(8) Å	α= 90°.
	b = 12.1908(5) Å	β= 90°.
	c = 9.1228(3) Å	γ = 90°.
Volume	2149.85(14) $Å^3$	
Z	4	
Density (calculated)	1.290 Mg/m^3	
Absorption coefficient	0.905 mm^{-1}	
F(000)	896	
Crystal size	0.360 x 0.040 x 0.030 mm^3	
Theta range for data collection	1.670 to 28.581°.	
Index ranges	-25<=h<=25, -16<=k<=16, -12<=l<=12	
Reflections collected	20760	
Independent reflections	5450 [R(int) = 0.0595]	
Completeness to theta = 25.000°	100.0 %	
Refinement method	Full-matrix least-squares on F^2	
Data / restraints / parameters	5450 / 1 / 225	
Goodness-of-fit on F^2	1.037	
Final R indices [I>2sigma(I)]	R1 = 0.0278, wR2 = 0.0541	
R indices (all data)	R1 = 0.0365, wR2 = 0.0574	
Absolute structure parameter	-0.010(6)	
Largest diff. peak and hole	0.239 and -0.427 $e.Å^{-3}$	

Table S6. Atomic coordinates (x 10^4) and equivalent isotropic displacement parameters ($Å^2$x 10^3) for [$Fe^{II}(S_2^{Me2}N_3(Pr,Pr)$]•••H-OMe (**1•••H-OMe**). U(eq) is defined as one third of the trace of the orthogonalized U^{ij} tensor.

	x	y	z	U(eq)
Fe(1)	3775(1)	3022(1)	4521(1)	12(1)
S(1)	4763(1)	2529(1)	5843(1)	18(1)
S(2)	2810(1)	3791(1)	5604(1)	16(1)
C(3)	5131(2)	429(2)	6602(3)	25(1)
C(2)	4162(2)	1310(3)	8013(3)	23(1)
C(16)	2605(2)	5953(2)	6249(3)	24(1)
N(2)	3653(1)	2996(2)	2174(2)	13(1)
N(3)	4030(1)	4726(2)	4216(2)	14(1)
C(8)	3414(2)	1944(2)	1551(3)	16(1)
C(7)	2831(1)	1469(2)	2473(3)	18(1)
C(6)	3084(1)	713(2)	3670(3)	17(1)
C(4)	3944(2)	662(2)	5511(3)	17(1)
C(5)	3805(2)	-543(2)	5702(3)	27(1)
C(1)	4492(2)	1172(2)	6492(3)	17(1)
C(9)	4239(2)	3450(2)	1316(3)	19(1)
C(10)	4362(2)	4657(2)	1610(3)	20(1)
C(11)	4584(1)	4942(2)	3157(3)	19(1)
C(12)	3732(1)	5469(2)	4970(3)	15(1)
C(13)	3892(2)	6679(2)	4895(3)	26(1)
C(14)	3191(1)	5119(2)	6101(3)	15(1)
C(15)	3567(2)	5006(2)	7583(3)	20(1)
C(18)	6536(2)	1817(3)	4486(6)	58(1)
O(1)	5954(2)	2000(2)	3601(3)	49(1)
N(1)	3612(1)	1253(2)	4584(3)	14(1)

Table S7. Bond lengths [Å] and angles [°] for [$Fe^{II}(S_2^{Me2}N_3(Pr,Pr)$]•••H-OMe (**1•••H-OMe**).

Fe(1)-N(3)	2.153(2)
Fe(1)-N(2)	2.154(2)
Fe(1)-N(1)	2.1802(19)
Fe(1)-S(2)	2.3103(7)
Fe(1)-S(1)	2.3372(8)
S(1)-C(1)	1.833(3)
S(2)-C(14)	1.837(3)
C(3)-C(1)	1.534(4)
C(3)-H(3A)	0.9800
C(3)-H(3B)	0.9800
C(3)-H(3C)	0.9800
C(2)-C(1)	1.536(4)
C(2)-H(2A)	0.9800
C(2)-H(2B)	0.9800
C(2)-H(2C)	0.9800
C(16)-C(14)	1.529(4)
C(16)-H(16A)	0.9800
C(16)-H(16B)	0.9800
C(16)-H(16C)	0.9800
N(2)-C(8)	1.477(3)
N(2)-C(9)	1.483(3)
N(2)-H(2)	1.0000
N(3)-C(12)	1.275(3)
N(3)-C(11)	1.466(3)
C(8)-C(7)	1.522(4)
C(8)-H(8A)	0.9900
C(8)-H(8B)	0.9900
C(7)-C(6)	1.510(4)
C(7)-H(7A)	0.9900
C(7)-H(7B)	0.9900
C(6)-N(1)	1.473(3)
C(6)-H(6A)	0.9900
C(6)-H(6B)	0.9900
C(4)-N(1)	1.283(3)

C(4)-C(5)	1.503(4)
C(4)-C(1)	1.520(4)
C(5)-H(5A)	0.9800
C(5)-H(5B)	0.9800
C(5)-H(5C)	0.9800
C(9)-C(10)	1.515(4)
C(9)-H(9A)	0.9900
C(9)-H(9B)	0.9900
C(10)-C(11)	1.515(4)
C(10)-H(10A)	0.9900
C(10)-H(10B)	0.9900
C(11)-H(11A)	0.9900
C(11)-H(11B)	0.9900
C(12)-C(13)	1.508(4)
C(12)-C(14)	1.530(4)
C(13)-H(13A)	0.9800
C(13)-H(13B)	0.9800
C(13)-H(13C)	0.9800
C(14)-C(15)	1.541(4)
C(15)-H(15A)	0.9800
C(15)-H(15B)	0.9800
C(15)-H(15C)	0.9800
C(18)-O(1)	1.401(5)
C(18)-H(18A)	0.9800
C(18)-H(18B)	0.9800
C(18)-H(18C)	0.9800
O(1)-H(1)	0.8400

N(3)-Fe(1)-N(2)	84.87(8)
N(3)-Fe(1)-N(1)	172.24(8)
N(2)-Fe(1)-N(1)	89.77(8)
N(3)-Fe(1)-S(2)	81.33(6)
N(2)-Fe(1)-S(2)	110.05(6)
N(1)-Fe(1)-S(2)	105.83(6)
N(3)-Fe(1)-S(1)	97.32(6)
N(2)-Fe(1)-S(1)	126.76(6)

N(1)-Fe(1)-S(1)	81.40(6)
S(2)-Fe(1)-S(1)	122.93(3)
C(1)-S(1)-Fe(1)	99.51(9)
C(14)-S(2)-Fe(1)	97.95(9)
C(1)-C(3)-H(3A)	109.5
C(1)-C(3)-H(3B)	109.5
H(3A)-C(3)-H(3B)	109.5
C(1)-C(3)-H(3C)	109.5
H(3A)-C(3)-H(3C)	109.5
H(3B)-C(3)-H(3C)	109.5
C(1)-C(2)-H(2A)	109.5
C(1)-C(2)-H(2B)	109.5
H(2A)-C(2)-H(2B)	109.5
C(1)-C(2)-H(2C)	109.5
H(2A)-C(2)-H(2C)	109.5
H(2B)-C(2)-H(2C)	109.5
C(14)-C(16)-H(16A)	109.5
C(14)-C(16)-H(16B)	109.5
H(16A)-C(16)-H(16B)	109.5
C(14)-C(16)-H(16C)	109.5
H(16A)-C(16)-H(16C)	109.5
H(16B)-C(16)-H(16C)	109.5
C(8)-N(2)-C(9)	111.1(2)
C(8)-N(2)-Fe(1)	115.43(16)
C(9)-N(2)-Fe(1)	115.86(16)
C(8)-N(2)-H(2)	104.3
C(9)-N(2)-H(2)	104.3
Fe(1)-N(2)-H(2)	104.3
C(12)-N(3)-C(11)	123.8(2)
C(12)-N(3)-Fe(1)	120.83(18)
C(11)-N(3)-Fe(1)	115.25(17)
N(2)-C(8)-C(7)	110.5(2)
N(2)-C(8)-H(8A)	109.6
C(7)-C(8)-H(8A)	109.6
N(2)-C(8)-H(8B)	109.6
C(7)-C(8)-H(8B)	109.6

H(8A)-C(8)-H(8B)	108.1
C(6)-C(7)-C(8)	113.0(2)
C(6)-C(7)-H(7A)	109.0
C(8)-C(7)-H(7A)	109.0
C(6)-C(7)-H(7B)	109.0
C(8)-C(7)-H(7B)	109.0
H(7A)-C(7)-H(7B)	107.8
N(1)-C(6)-C(7)	111.2(2)
N(1)-C(6)-H(6A)	109.4
C(7)-C(6)-H(6A)	109.4
N(1)-C(6)-H(6B)	109.4
C(7)-C(6)-H(6B)	109.4
H(6A)-C(6)-H(6B)	108.0
N(1)-C(4)-C(5)	122.4(2)
N(1)-C(4)-C(1)	120.4(2)
C(5)-C(4)-C(1)	117.2(2)
C(4)-C(5)-H(5A)	109.5
C(4)-C(5)-H(5B)	109.5
H(5A)-C(5)-H(5B)	109.5
C(4)-C(5)-H(5C)	109.5
H(5A)-C(5)-H(5C)	109.5
H(5B)-C(5)-H(5C)	109.5
C(4)-C(1)-C(3)	110.9(2)
C(4)-C(1)-C(2)	106.7(2)
C(3)-C(1)-C(2)	109.8(2)
C(4)-C(1)-S(1)	112.23(18)
C(3)-C(1)-S(1)	108.9(2)
C(2)-C(1)-S(1)	108.17(19)
N(2)-C(9)-C(10)	112.9(2)
N(2)-C(9)-H(9A)	109.0
C(10)-C(9)-H(9A)	109.0
N(2)-C(9)-H(9B)	109.0
C(10)-C(9)-H(9B)	109.0
H(9A)-C(9)-H(9B)	107.8
C(9)-C(10)-C(11)	115.6(2)
C(9)-C(10)-H(10A)	108.4

C(11)-C(10)-H(10A)	108.4
C(9)-C(10)-H(10B)	108.4
C(11)-C(10)-H(10B)	108.4
H(10A)-C(10)-H(10B)	107.4
N(3)-C(11)-C(10)	111.5(2)
N(3)-C(11)-H(11A)	109.3
C(10)-C(11)-H(11A)	109.3
N(3)-C(11)-H(11B)	109.3
C(10)-C(11)-H(11B)	109.3
H(11A)-C(11)-H(11B)	108.0
N(3)-C(12)-C(13)	125.3(2)
N(3)-C(12)-C(14)	118.3(2)
C(13)-C(12)-C(14)	116.3(2)
C(12)-C(13)-H(13A)	109.5
C(12)-C(13)-H(13B)	109.5
H(13A)-C(13)-H(13B)	109.5
C(12)-C(13)-H(13C)	109.5
H(13A)-C(13)-H(13C)	109.5
H(13B)-C(13)-H(13C)	109.5
C(16)-C(14)-C(12)	112.4(2)
C(16)-C(14)-C(15)	109.4(2)
C(12)-C(14)-C(15)	107.1(2)
C(16)-C(14)-S(2)	108.03(19)
C(12)-C(14)-S(2)	110.74(18)
C(15)-C(14)-S(2)	109.10(18)
C(14)-C(15)-H(15A)	109.5
C(14)-C(15)-H(15B)	109.5
H(15A)-C(15)-H(15B)	109.5
C(14)-C(15)-H(15C)	109.5
H(15A)-C(15)-H(15C)	109.5
H(15B)-C(15)-H(15C)	109.5
O(1)-C(18)-H(18A)	109.5
O(1)-C(18)-H(18B)	109.5
H(18A)-C(18)-H(18B)	109.5
O(1)-C(18)-H(18C)	109.5
H(18A)-C(18)-H(18C)	109.5

H(18B)-C(18)-H(18C)	109.5
C(18)-O(1)-H(1)	109.5
C(4)-N(1)-C(6)	117.9(2)
C(4)-N(1)-Fe(1)	120.06(18)
C(6)-N(1)-Fe(1)	121.85(16)

*Symmetry transformations used to generate equivalent atoms.

Table S8. Anisotropic displacement parameters ($Å^2 x\ 10^3$) for [$Fe^{II}(S_2^{Me2}N_3(Pr,Pr)$]•••H-OMe (**1•••H-OMe**). The anisotropicdisplacement factor exponent takes the form: $-2\pi^2[\ h^2a^{*2}U^{11} + ... + 2\ h\ k\ a^*\ b^*\ U^{12}\ ]$

	U^{11}	U^{22}	U^{33}	U^{23}	U^{13}	U^{12}
Fe(1)	12(1)	12(1)	11(1)	0(1)	0(1)	0(1)
S(1)	16(1)	17(1)	21(1)	0(1)	-5(1)	1(1)
S(2)	13(1)	16(1)	18(1)	-3(1)	4(1)	-3(1)
C(3)	23(2)	24(2)	26(2)	3(1)	0(1)	7(1)
C(2)	24(2)	28(2)	16(1)	0(1)	-1(1)	2(1)
C(16)	16(2)	20(2)	35(2)	-10(1)	-1(1)	4(1)
N(2)	12(1)	16(1)	12(1)	0(1)	0(1)	2(1)
N(3)	12(1)	17(1)	13(1)	2(1)	1(1)	-2(1)
C(8)	18(2)	18(1)	14(1)	-3(1)	-1(1)	1(1)
C(7)	18(2)	19(1)	16(1)	-3(1)	-4(1)	0(1)
C(6)	19(2)	15(1)	18(1)	-2(1)	-1(1)	-4(1)
C(4)	21(1)	15(1)	14(1)	-1(1)	3(1)	2(1)
C(5)	41(2)	15(1)	24(2)	5(1)	-6(1)	0(1)
C(1)	19(2)	16(1)	16(1)	1(1)	1(1)	5(1)
C(9)	18(2)	25(2)	16(1)	0(1)	5(1)	-1(1)
C(10)	19(2)	24(2)	16(1)	5(1)	5(1)	-4(1)
C(11)	16(2)	22(2)	19(1)	2(1)	4(1)	-5(1)
C(12)	13(1)	13(1)	18(1)	1(1)	-3(1)	-2(1)
C(13)	29(2)	15(1)	36(2)	0(1)	3(1)	-3(1)
C(14)	14(1)	14(1)	19(1)	-2(1)	0(1)	0(1)
C(15)	19(2)	23(2)	17(1)	-3(1)	0(1)	-2(1)
C(18)	43(2)	59(3)	72(2)	-23(3)	22(3)	-25(2)
O(1)	60(2)	49(2)	39(2)	-13(1)	24(1)	-4(1)
N(1)	16(1)	14(1)	13(1)	0(1)	1(1)	-1(1)

Table S9. Hydrogen coordinates (x 10^4) and isotropic displacement parameters ($Å^2$x 10^3) for [$Fe^{II}(S_2^{Me2}N_3(Pr,Pr)$]•••H-OMe (**1•••H-OMe**).

	x	y	z	U(eq)
H(3A)	5003	-259	7088	37
H(3B)	5491	800	7173	37
H(3C)	5305	271	5616	37
H(2A)	3783	1841	7955	34
H(2B)	4512	1574	8707	34
H(2C)	3982	601	8349	34
H(16A)	2792	6655	6589	35
H(16B)	2264	5683	6959	35
H(16C)	2381	6055	5295	35
H(2)	3263	3516	1983	16
H(8A)	3804	1419	1519	20
H(8B)	3250	2062	536	20
H(7A)	2567	2078	2924	21
H(7B)	2511	1058	1826	21
H(6A)	2689	489	4292	21
H(6B)	3284	43	3224	21
H(5A)	3304	-673	5676	40
H(5B)	3990	-787	6647	40
H(5C)	4028	-953	4908	40
H(9A)	4144	3346	259	23
H(9B)	4664	3035	1558	23
H(10A)	3931	5062	1386	24
H(10B)	4723	4921	924	24
H(11A)	4997	4505	3421	23
H(11B)	4713	5728	3201	23
H(13A)	4328	6790	4367	40
H(13B)	3934	6973	5890	40
H(13C)	3518	7059	4379	40
H(15A)	3765	5716	7862	29
H(15B)	3938	4462	7495	29

H(15C)	3237	4769	8334	29
H(18A)	6519	2305	5339	87
H(18B)	6957	1968	3921	87
H(18C)	6540	1052	4815	87
H(1)	5603	2078	4134	74

Table S10. DFT optimized bond lengths (using the B3LYP functional and def2-TZVP basis set) versus experimental distances for [$Fe^{II}(S_2^{Me2}N_3(Pr,Pr)$]•••H-OMe (**1•••H-OMe**) containing a MeOH solvent molecule H-bonded to one of the thiolate sulfurs, S(2).

Bond	Calcd Bond Length (Å)	Exptl Bond Length (Å)
Fe-S(1)	2.338	2.3103(7)
Fe-S(2)	2.356	2.3372(8)
Fe-N(1)	2.194	2.1802(19)
Fe-N(2)	2.165	2.154(2)
Fe-N(3)	2.185	2.153(2)
S(2)•••H	2.224	2.318
O(1)-H	0.985	0.840
τ	0.78	0.76

Table S11. DFT optimized bond lengths (using the B3LYP functional and def2-TZVP basis set) versus experimental distances for [$Fe^{II}(S_2^{Me2}N_3(Pr,Pr)$] (**1**).

Bond	Calcd Bond Length (Å)	Exptl Bond Length (Å)
Fe-S(1)	2.338	2.3263(5)
Fe-S(2)	2.336	2.3306(5)
Fe-N(1)	2.184	2.1556(16)
Fe-N(2)	2.203	2.1656(16)
Fe-N(3)	2.174	2.1815(15)
τ	0.79	0.79

Table S12. DFT optimized bond lengths (using the B3LYP functional and def2-TZVP basis set) for [$Fe^{III}(S_2^{Me2}N_3(Pr,Pr)(O_2)$] (**2**) in MeOH.

Bond	Calcd Bond Length (Å)
Fe-S(1)	2.241
Fe-S(2)	2.266
Fe-N(1)	1.999
Fe-N(2)	2.118
Fe-N(3)	1.996
Fe-O(1)	1.973
O(1)-O(2)	1.310

Table S13. DFT optimized coordinates (using the B3LYP functional and def2-TZVP basis set) for $[Fe^{II}(S_2^{Me2}N_3(Pr,Pr)]$•••H-OMe (**1•••H-OMe**) in MeOH

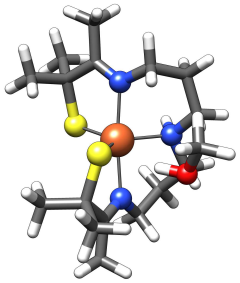

Fe	0.187840000	0.031874000	2.207628000
S	2.516433000	0.158277000	2.542709000
S	-1.087148000	1.968776000	1.908785000
N	0.218245000	-0.269054000	4.372063000
N	0.206799000	0.078130000	0.042963000
N	-1.000941000	-1.793120000	1.941660000
O	2.537274000	-3.021609000	2.951929000
H	2.470473000	-2.044771000	2.848378000
C	3.382440000	-3.497198000	1.912449000
C	-1.458421000	-2.393969000	3.211330000
C	0.067044000	1.266016000	-2.096312000
C	2.518161000	0.562024000	4.350048000
C	-0.409893000	-2.797316000	1.031673000
C	3.742861000	-0.114823000	4.988821000
C	-0.259649000	-2.294192000	-0.398245000
C	0.711017000	-1.128021000	-0.601647000
C	-0.107098000	1.131375000	-0.602170000
H	-2.314984000	3.715220000	0.016495000
H	-2.683419000	2.101621000	-0.601732000
H	-1.710854000	3.226931000	-1.566366000
H	-1.425665000	0.120974000	5.626442000
H	-2.504589000	-0.548820000	3.557839000
H	0.081005000	4.324113000	0.639446000
H	-2.799208000	-1.773363000	4.775403000
H	0.305437000	0.604831000	6.912920000
H	1.772279000	2.583192000	4.033897000
H	-0.697003000	-1.466463000	5.829725000
H	0.716525000	3.712487000	-0.893226000
H	2.636691000	2.375830000	5.569669000
H	1.338761000	3.079669000	0.643204000
H	2.070031000	0.688456000	6.957514000
H	-1.821357000	-1.403575000	1.480762000
H	-0.675368000	0.656593000	-2.617278000
H	-2.212233000	-3.158952000	2.998669000
H	1.253899000	-0.875223000	6.947679000
H	-0.052192000	2.292777000	-2.426167000
H	3.537154000	2.446021000	4.049530000
H	-0.603739000	-2.897794000	3.667538000
H	-1.241104000	-2.012344000	-0.793346000
H	1.053582000	0.921820000	-2.405648000

H	3.875139000	0.176652000	6.031987000
H	-1.043927000	-3.691968000	1.021694000
H	0.885828000	-0.997917000	-1.669493000
H	0.557774000	-3.086203000	1.444010000
H	4.637113000	0.183937000	4.442100000
H	3.658076000	-1.200769000	4.937644000
H	1.669173000	-1.370957000	-0.134165000
H	0.094287000	-3.131944000	-1.003552000
C	1.239191000	0.102947000	5.045455000
H	2.950831000	-3.313503000	0.921927000
H	4.372631000	-3.030736000	1.949640000
H	3.499975000	-4.573265000	2.043241000
C	-0.981308000	-0.718954000	5.083156000
C	1.224795000	0.143659000	6.550458000
C	0.445014000	3.432735000	0.128148000
C	-2.021127000	-1.329622000	4.151331000
C	-0.651344000	2.350094000	0.144792000
C	-1.916522000	2.875921000	-0.553424000
C	2.617569000	2.090501000	4.514826000

Table S14. DFT optimized coordinates (using the B3LYP functional and def2-TZVP basis set) for $[Fe^{II}(S_2^{Me2}N_3(Pr,Pr)]$ (**1**)

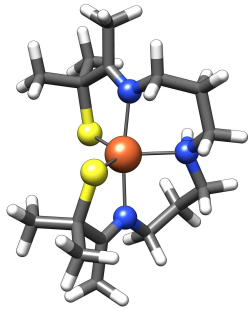

Fe	0.151055000	-0.153370000	-0.036351000
S	2.477303000	-0.250168000	-0.247789000
S	-1.247675000	-1.997855000	0.278330000
N	0.269386000	0.057142000	-2.206808000
N	-0.928519000	1.763793000	0.070718000
N	0.016241000	-0.069024000	2.132000000
C	2.568112000	-0.747811000	-2.028832000
C	1.322739000	-0.339939000	-2.811064000
C	-1.028758000	-2.264901000	2.101089000
C	-0.433209000	-1.049130000	2.811087000
C	-1.306898000	2.304878000	-1.249418000
C	-1.921562000	1.215370000	-2.127842000
C	-0.897945000	0.475340000	-2.984013000
C	-0.252421000	2.761692000	0.923418000
C	-0.231228000	2.365651000	2.394932000
C	0.589982000	1.121986000	2.745249000
C	1.379951000	-0.457950000	-4.312116000
C	-0.374488000	-1.097541000	4.320683000
H	-1.786078000	1.479348000	0.539604000
H	-2.006129000	3.137244000	-1.116387000
H	-0.404878000	2.709552000	-1.713902000
H	-2.463002000	0.510480000	-1.491398000
H	-2.657319000	1.660370000	-2.800446000
H	0.471149000	-0.922202000	-4.696208000
H	-0.578503000	1.135086000	-3.796011000
H	0.765694000	2.886930000	0.546971000
H	-0.759661000	3.729426000	0.828449000
H	0.182384000	3.206604000	2.956476000
H	-1.258579000	2.226426000	2.747786000
H	0.667812000	1.048144000	3.830167000
H	1.601133000	1.235294000	2.344946000
H	-1.367235000	-0.398653000	-3.447039000
H	2.233819000	-1.038332000	-4.646162000
H	1.451765000	0.537169000	-4.760971000
H	0.634024000	-0.881032000	4.673977000
H	-0.666809000	-2.068104000	4.707096000
H	-1.043417000	-0.347712000	4.749274000
C	2.690446000	-2.281797000	-2.113409000
H	4.686319000	-0.355270000	-2.048674000

C	-0.063159000	-3.446644000	2.314498000
C	-2.405733000	-2.598468000	2.700653000
H	0.911188000	-3.226919000	1.877278000
H	0.071283000	-3.671117000	3.375967000
H	-0.466931000	-4.334254000	1.827358000
H	-2.833516000	-3.442679000	2.160180000
H	-2.341056000	-2.873266000	3.755383000
H	-3.086418000	-1.751708000	2.601763000
H	1.824992000	-2.759595000	-1.653823000
C	3.814067000	-0.089487000	-2.645613000
H	2.769948000	-2.620712000	-3.150061000
H	3.994014000	-0.423263000	-3.669356000
H	3.719258000	0.997255000	-2.643714000
H	3.585638000	-2.602131000	-1.580285000

Table S15. DFT optimized coordinates (using the B3LYP functional and def2-TZVP basis set) for $[Fe^{III}(S_2^{Me2}N_3(Pr,Pr)(O_2)]$ (**2**) in MeOH

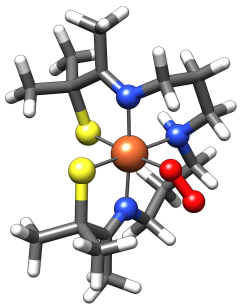

Fe	0.070175000	-0.233500000	0.011578000
S	2.292906000	-0.517674000	-0.018409000
S	-0.449790000	-2.407961000	0.382216000
N	0.135832000	-0.490511000	-1.969385000
N	-1.957531000	0.348280000	0.196171000
N	0.074661000	-0.129327000	2.004716000
O	0.423965000	1.693274000	-0.225298000
O	0.040972000	2.280132000	-1.331942000
C	2.575821000	-0.501265000	-1.839479000
C	1.258572000	-0.543855000	-2.586763000
C	0.050558000	-2.548595000	2.155468000
C	0.110917000	-1.160264000	2.764134000
C	-2.694983000	0.452799000	-1.077509000
C	-2.385408000	-0.700666000	-2.014831000
C	-1.086798000	-0.548183000	-2.787931000
C	-2.212466000	1.551055000	1.026887000
C	-1.673053000	1.473994000	2.449417000
C	-0.170081000	1.199792000	2.563334000
C	1.332525000	-0.628989000	-4.086691000
C	0.170415000	-1.070641000	4.265610000
H	-2.309651000	-0.468746000	0.691134000
H	-3.767867000	0.490946000	-0.863137000
H	-2.414395000	1.399167000	-1.541466000
H	-2.402536000	-1.644329000	-1.465902000
H	-3.181769000	-0.757172000	-2.760614000
H	-1.138645000	0.369118000	-3.381620000
H	-1.004277000	-1.380037000	-3.489884000
H	-1.776991000	2.400236000	0.505117000
H	-3.294487000	1.713908000	1.073684000
H	-1.892126000	2.428470000	2.933628000
H	-2.210738000	0.702060000	3.007945000
H	0.136582000	1.272178000	3.604324000
H	0.395541000	1.926528000	1.986057000
H	0.903998000	-1.571500000	-4.436135000
H	2.354250000	-0.567632000	-4.445349000
H	0.754751000	0.176709000	-4.543585000
H	0.880396000	-0.310620000	4.588255000
H	0.466201000	-2.021550000	4.698588000
H	-0.809582000	-0.808184000	4.671969000
C	3.417715000	-1.737443000	-2.204058000

C	3.334217000	0.783135000	-2.224960000
C	1.414456000	-3.245734000	2.284161000
C	-1.023372000	-3.383370000	2.876879000
H	2.176705000	-2.702423000	1.729328000
H	1.718583000	-3.318269000	3.331704000
H	1.340323000	-4.257055000	1.882425000
H	-1.151241000	-4.325533000	2.343126000
H	-0.734413000	-3.616256000	3.903350000
H	-1.982428000	-2.864422000	2.888685000
H	2.874527000	-2.655404000	-1.977468000
H	4.335459000	-1.727824000	-1.615154000
H	3.695558000	-1.743015000	-3.259871000
H	3.572045000	0.803138000	-3.290967000
H	2.745451000	1.665750000	-1.978736000
H	4.271337000	0.824032000	-1.669282000

Reference

1. M. N. Blakely, M. A. Dedushko, P. C. Y. Poon, G. Villar-Acevedo and J. A. Kovacs, Formation of a Reactive, Alkyl Thiolate-Ligated FeIII-Superoxo Intermediate Derived from Dioxygen, *J. Am. Chem. Soc.*, 2019, **141**, 1867-1870.
2. J. J. N. Ellison, A.; Shoner, S. C.; Barnhart, D.; Cowen, J. A., Kovacs, J. A., Reactivity of Five-Coordinate Models for the Thiolate-Ligated Fe Site of Nitrile Hydratase, *J. Am. Chem. Soc.*, 1998, **120**, 5691-5700.
3. F. E. Grubbs, Procedures for Detecting Outlying Observations in Samples, *Technometrics*, 1969, **11**, 1-21.
4. Kinetic Studio,(5.1.0.6), TgK Scientific, Salisbury, UK,2018.
5. S. V. Kryatov, E. V. Rybak-Akimova and S. Schindler, Kinetics and Mechanisms of Formation and Reactivity of Non-heme Iron Oxygen Intermediates, *Chemical reviews*, 2005, **105**, 2175-2226.
6. F. Neese, The ORCA program system, *Comput. Molec. Sci.*, 2012, **2**, 73-78.
7. S. E. Grimme, S.; Goerigk, L., *J. Comput. Chem*, 2011, **32**, 1456-1465.
8. V. C. Barone, M., Quantum Calculation of Molecular Energies and Energy Gradients in Solution by a Conductor Solvent Model, *J. Phys. Chem.*, 1998, **102**, 1995 -2001.
9. C. B. Adamo, V., Toward reliable density functional methods without adjustable parameters: The PBE0 model, *J. Chem. Phys.*, 1999, **110**, 6158 – 6170.
10. F. W. Neese, F.; Hansen, A.; Becker, U., Efficient, approximate and parallel Hartree-Fock and hybrid DFT calculations. A 'chain-of-spheres' algorithm for the Hartree-Fock exchange, *Chem. Phys.*, 2009, **356**, 98–109.
11. S. H.-G. Hirata, M., Time-dependent density functional theory within the Tamm–Dancoff approximation, *Chem. Phys. Lett.*, 1999, **314**, 291–299.
12. F. O. Neese, G., Efficient use of the resolution of the identity approximation in time-dependent density functional calculations with hybrid density functionals, *Chem. Phys. Lett.*, 2002, **362**, 170–178.
13. E. F. G. Pettersen, T. D.; Huang, C. C.; Couch, G. S.; Greenblatt, D. M.; Meng, E. C.; Ferrin, T. E., UCSF Chimera- a visualization system for exploratory research and analysis, *J. Comput. Chem.*, 2004, **25**, 1605–1612.
14. S. V. A. Bruker. APEX2 (Version 2.1-4), SADABS (Version 2007/4). 2007.
15. G. Sheldrick, A short history of SHELX, *Acta Crystallographica Section A*, 2008, **64**, 112-122.
16. G. Sheldrick, Crystal structure refinement with SHELXL, *Acta Crystallographica Section C*, 2015, **71**, 3-8.
17. G. M. Sheldrick, SHELXL-97, Program for the Solution of Crystal Structures University of Göttingen, Germany,1997.
18. D. K. Waasmaier, A., *Acta Crystallogr. A.*, 1995, **51**, 416.
19. L. Farrugia, WinGX and ORTEP for Windows: an update, *Journal of Applied Crystallography*, 2012, **45**, 849-854.
20. D. S. BIOVIA, BIOVIA Discovery Studio Dassault Systèmes, San Diego,2020.
21. J. H. Espenson, *Chemical Kinetics and Reaction Mechanisms*, McGraw-Hill, New York, 1981.